

Classical and quantum study of the motion of a particle in a gravitational field

Mário N. Berberan-Santos

Centro de Química-Física Molecular, Instituto Superior Técnico, P-1049-001 Lisboa, Portugal
E-mail: berberan@mail.ist.utl.pt

Evgeny N. Bodunov

Physical Department, Petersburg State Transport University, St. Petersburg, Russia
E-mail: bodunov@mail.admiral.ru

Lionello Pogliani*

Dipartimento di Chimica, Università della Calabria, I-87030 Rende (CS), Italy
E-mail: lionp@unical.it

Received 13 August 2004; revised 7 September 2004

The classical and the quantum mechanical description of a one-dimensional motion of a particle in the presence of a gravitational field is thoroughly discussed. The attention is centered on the evolution of classical and quantum mechanical position probability distribution function. The classical case has been compared with three different quantum cases: (a) a quantum stationary case, (b) a quantum non-stationary zero approximation case, where the wave packet has the shape of the first eigenfunction, and (c) a quantum non-stationary general case, where the wave packet is a superposition of stationary states.

KEY WORDS: motion of a particle, gravitation, classical case, quantum case

1. Introduction

Textbooks and pedagogical articles on quantum mechanics present various formulations for the connection between the Schrödinger wave function and the classical motion of particle [1]. For free particles Gaussian wave packets constructed from plane wave solutions are frequently discussed as an analytic example. For bound states, instead, wave packet solution for the harmonic oscillator problem can be constructed, which exhibit the classical periodicity of the

*Current address: Facultad de Farmacia, Dept. Química Física, Universidad de Valencia, Av. V.A. Estelles s/n, 46100 Burjassot (Valencia), Spain.

particle motion. Numerical solutions of the Schrödinger equation representing wave packet scattering events have extensively been studied and they help to visualize the time dependence of such interaction [1–4].

A familiar approach for stationary state solution is to compare the probability density, given by $P_{\text{qu}}^{(\text{st})}(x, n) = |\psi_n(x)|^2$, with a classical probability distribution, $P_{\text{cl}}(x)$, and show that the two probabilities approach each other in the limit of large quantum number n , and this is often done using the harmonic oscillator as an example. The agreement between the classical and the modified quantum probability densities [2], $P_{\text{qu}}(x)$, is very good. In fact, quantum effects become noticeable only in the region near the potential barrier, where the particle can penetrate through the barrier. The great attention devoted to the simple harmonic oscillator in classical, statistical, and quantum mechanics is certainly due to its direct connection with important physical systems from elementary classical mechanics to quantum field theory.

An important example of linear potential is the gravitational field, which plays an interesting role in our life, as has recently been underlined for the case of a gas in a gravitational field [5–7]. The last of these articles concerned the effect that a constant gravitational field had on the existence and position of the liquid–vapor boundary of a pure classical fluid. Here, the cases of a perfect gas and incompressible liquid model, as well as of a van der Waals fluid model were analysed. Linear potentials are also important in the field of elementary particle physics, in fact, it is argued that at large separations the quark–antiquark interaction is described by a linear potential.

The solution of the Schrödinger equation for particle bouncing on perfectly reflecting surface under the influence of gravity, known as “The quantum bouncer” problem [8], is discussed in a number of textbooks. The study of the dynamics of a bouncing wave packet, initially Gaussian in shape, in a linear potential is very interesting from a pedagogical standpoint, as it underlines some of the differences between classical and quantum dynamics [8–16]. The classical motion is periodic, since no energy dissipation is assumed to take place, and it repeats itself indefinitely, while the quantum motion is aperiodic, and exhibits interesting collapses and revivals of the oscillations, similar to those observed in many other quantum systems. In spite of this, there is a clear correspondence between the classical and quantum limits.

The subject of this paper will be to draw a comparison between the classical, $P_{\text{cl}}(x)$, and the modified quantum probability densities, $P_{\text{qu}}(x)$, which, so far, have not been compared. Some aspects of the quantum bouncer problem have practical implications, e.g., the condensation phenomena of an ideal Bose–Einstein gas [17,18], and the observation of quantum states of neutrons in Earth’s gravitational field [19]. In recent years, the development of high precision techniques to cool and manipulate atoms and neutrons allowed to develop an experimental version of the simple quantum bouncer [20 and references therein].

Last but not least, the exact solution of the Schrödinger equation in a linear potential is connected with name of an outstanding scientist, who lived well before Schrödinger, George Biddel Airy. For the interested reader a short bibliographic note is given at the end of the paper.

2. Classical description

2.1. Equation of motion

The potential energy of a particle of mass m in a gravitational field pointing in the $-x$ direction, where it is subjected to a constant force ($F(x) = mg$), is given by

$$V(x) = mgx, \quad (1)$$

where g is the gravitational acceleration. In classical mechanics, the equation of particle motion reads

$$\frac{d^2}{dt^2}x(t) = -g. \quad (2)$$

If the particle is falling down from some maximum height, x_{\max} , the classical turning point, with zero speed

$$x(0) = x_{\max} \quad \text{and} \quad \frac{d}{dt}x(t)|_{t=0} = 0 \quad (3)$$

then the solution of equation (2) has the form

$$x(t) = x_{\max} - \frac{gt^2}{2}. \quad (4)$$

In the case of elastic reflection of the particle at the Earth surface ($V(x) = \infty$ for $x < 0$), the motion is periodic and is limited inside the interval $[0, x_{\max}]$. The period of this motion, T , can be obtained from the condition $x(T/2) = 0$, and is equal to, $T = (8x_{\max}/g)^{1/2}$. Maximum height, x_{\max} , is reached at time $t = T + nTn = 0, 1, 2, \dots$ (see figure 1), when all kinetic energy is transferred into potential energy, $mv_{\max}^2/2 = mgx_{\max}$, i.e. $x_{\max} = v_{\max}^2/2g$, where v_{\max} is the maximum speed of the particle. Thus, the particle motion in the gravitation field is periodical. With the given result, $T = (8x_{\max}/g)^{1/2}$, equation (4) can be rewritten, within the time interval $[0, T]$, as

$$x(t)/x_{\max} = |1 - 4(t/T)^2|. \quad (5)$$

This function is shown in figure 1.

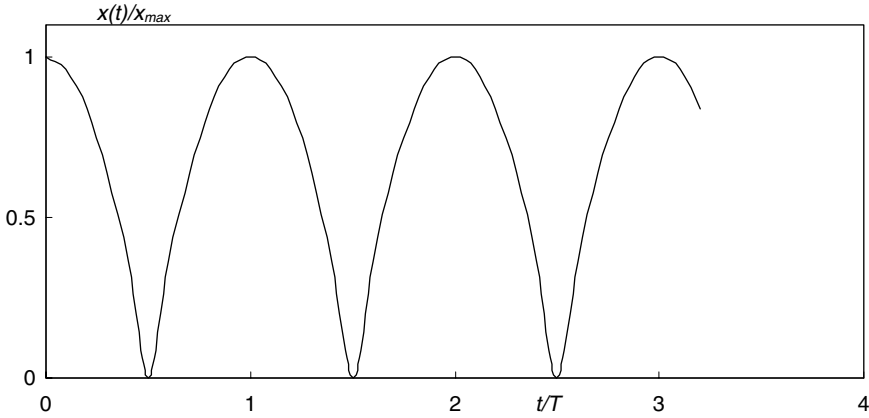


Figure 1. Trajectory of particle motions in the gravitational field.

2.2. The classical position probability density

The classical position probability density for this oscillator can be obtained by two ways. One way was described in Refs. [3,5]. The average value of a function of the position coordinate, $\langle f(x) \rangle$, can be obtained as

$$\begin{aligned} \langle f(x) \rangle &= \frac{1}{T} \int_0^T f(x(t)) dt = \frac{1}{T} \int_0^T f(x(t)) \frac{dx}{dx/dt} \\ &\rightarrow \frac{2}{T} \int_0^{x_{\max}} f(x) \frac{dx}{v(x)} = \int_0^{x_{\max}} f(x) P_{\text{cl}}(x) dx, \end{aligned} \quad (6)$$

where, $v(x) = dx/dt$, and $P_{\text{cl}}(x) = 2/Tv(x)$ is the classical position probability distribution. The integral is taken between the turning points 0 and x_{\max} that covers to only half the period, $T/2$. The local speed is related to the potential energy function via

$$E = \frac{1}{2}mv^2(x) + V(x), \quad (7)$$

where E is total energy of the oscillator. Taking into account that $E = mgx_{\max}$ and using equations: $T = (8x_{\max}/g)^{1/2}$, $P_{\text{cl}}(x) = 2/Tv(x)$, and (7), one gets

$$P_{\text{cl}}(x) = \frac{1}{2} \frac{1}{\sqrt{x_{\max}(x_{\max} - x)}}. \quad (8)$$

But another way of obtaining the classical position probability density in the presence of a gravitational field was suggested some years ago [2]. $P_{\text{cl}}(x)$ can be obtained as

$$P_{\text{cl}}(x) = \frac{1}{T} \int_0^T \delta(x - x_{\max} + \frac{1}{2}gt^2) dt. \quad (9)$$

This integral can be evaluated expressing the δ function of a function $y(t)$ as [21]

$$\delta(y(t)) = \sum_i \frac{\delta(t - t_i)}{|dy/dt|_{t=t_i}}. \tag{10}$$

Here the sum is over all simple zeros t_i of $y(t)$. For fixed $0 < x < x_{\max}$, the function

$$y(t) = x - x_{\max} + \frac{1}{2}gt^2 \tag{11}$$

has two simple zeros $t_{1,2}(x - x_{\max} + 0.5gt_{1,2}^2 = 0)$ along the interval of integration $[0, T]$, namely,

$$t_{1,2} = \pm \sqrt{\frac{2(x_{\max} - x)}{g}} \tag{12}$$

and

$$|dy/dt|_{t=t_{1,2}} = |gt|_{t=t_{1,2}} = g\sqrt{\frac{2x_{\max} - 2x}{g}} = \sqrt{2g(x_{\max} - x)}. \tag{13}$$

Hence, for $0 < x < x_{\max}$, equation (9) becomes

$$P_{cl}(x) = \frac{1}{T} \int_0^T \sum_{i=1,2} \frac{\delta(t - t_i)}{\sqrt{2g(x_{\max} - x)}} dt = \frac{1}{T} \frac{2}{\sqrt{2g(x_{\max} - x)}} = \frac{1}{2} \frac{1}{\sqrt{x_{\max}(x_{\max} - x)}}. \tag{14}$$

Hence we obtain the result of the preceding paragraph [see equation (8)]. Finally, for $x < 0$ and $x > x_{\max}$, function (11) has no zeros in the interval $[0, T]$, and the integral (9) is equal to zero.

Thus, the classical position probability density for the particle in a gravitational field is

$$P_{cl}(x) = \begin{cases} (1/2)[x_{\max}(x_{\max} - x)]^{-1/2}, & 0 < x < x_{\max}; \\ 0, & x < 0, x > x_{\max}. \end{cases} \tag{15}$$

The reader can check that the normalization condition, $\int_0^{x_{\max}} P_{cl}(x)dx = 1$, is fulfilled. This probability distribution is shown in figure 2 (dotted line), together with a quantum result from section 3.

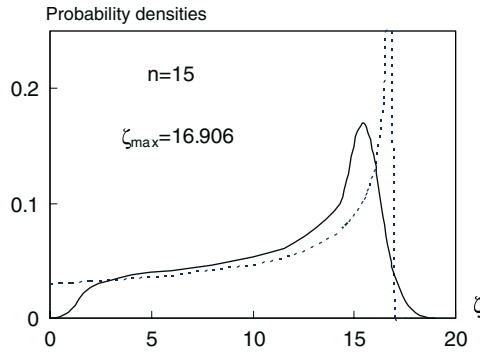


Figure 2. Classical, $P_{cl}(\zeta)$, dotted curve, and zero approximation quantum, $P_{qu}^{(0)}(\zeta)$, solid curve, position probability densities. $\zeta = x \left(\frac{2m^2g}{\hbar^2} \right)^{1/3}$.

3. Quantum mechanical description

3.1. Schrödinger equation and stationary wavefunction

The separated time-independent Schrödinger equation for a single particle is the same for y and z motions as in the field-free case, while for motion along the x direction we have the equation

$$\frac{d^2\varphi}{dx^2} + \frac{2m}{\hbar^2}(E - mgx)\varphi = 0. \quad (16)$$

The stationary wavefunction $\varphi(x)$ must obey the following boundary conditions: $\varphi(x) = 0$ for $x = 0$ and $\varphi(x) \rightarrow 0$ for $x \rightarrow \infty$. With the introduction of the following dimensionless height, and maximum height, which can also be read as a dimensionless energy,

$$\zeta = x \left(\frac{2m^2g}{\hbar^2} \right)^{1/3}, \quad \zeta_E = \frac{E}{mg} \left(\frac{2m^2g}{\hbar^2} \right)^{1/3} = x_{\max} \left(\frac{2m^2g}{\hbar^2} \right)^{1/3} \quad (17)$$

the Schrödinger equation (16) can be rewritten as

$$\frac{d^2\varphi}{d\zeta^2} - (\zeta - \zeta_E)\varphi = 0. \quad (18)$$

The following Airy function [21] is a solution of this equation for the given boundary condition,

$$\varphi_E(\zeta) = B_E \times Ai(\zeta - \zeta_E). \quad (19)$$

Here, the constant B_E can be obtained from the normalization condition, $\int_0^\infty \varphi_E^2(\zeta) d\zeta = 1$.

Table 1
Values of several roots of equation (20), of B_n , C_n , and C_n^2 .

n	ζ_n	B_n^2	C_n	C_n^2
1	2.3381	2.0338	0	0
12	14.5278	0.8242	0.1316	0.0173
13	15.3410	0.8021	0.2980	0.0888
14	16.1329	0.7821	0.5065	0.2566
15	16.9059	0.7640	0.6129	0.3835
16	17.6616	0.7475	0.4611	0.2126
17	18.4014	0.7323	0.1118	0.0125
18	19.1264	0.7183	-0.1224	0.0150

The wavefunction, φ_E , must obey the boundary condition $\varphi_E(\zeta = 0) = 0$. This condition allows to obtain the eigenvalues of the Schrödinger equation, through an equation, which is equivalent to the equation for deriving the roots of the Airy function [21–23],

$$J_{1/3} \left(\frac{2}{3} \zeta_E^{3/2} \right) + J_{-1/3} \left(\frac{2}{3} \zeta_E^{3/2} \right) = 0, \quad (20)$$

where $J_{1/3}$ and $J_{-1/3}$ are the Bessel functions of order $1/3$ and $-1/3$, respectively. Equation (20) has the following approximate solutions [9, 12, 18, 22, 23]

$$y_n = \frac{2}{3} \zeta_n^{3/2} \cong \pi \left(n - \frac{1}{4} \right), \quad n = 1, 2, \dots \quad (21)$$

The values of several roots of equation (20) (for $n \leq 10$) can be found in Refs. [1, 2, 14]. The values for $n = 1$ and $n > 11$ are shown in table 1.

The values of B_{En} [see equation (19)] for different n were calculated by numerical integration of the normalization condition for $\varphi_{En}(\zeta)$, and are also given in table 1. All the eigenfunctions $\varphi_n(\zeta) = B_n \text{Ai}(\zeta - \zeta_n)$ ($0 \leq \zeta < \infty$, to avoid using many subscripts subscript E has been dropped) are dependent on the Airy function $\text{Ai}(\zeta)$, whose plot can be found in Refs. [2, 10, 14].

If the particle is in a quantum stationary state n , its position probability density, $P_{\text{qu}}^{(\text{st})}(\zeta)$, is obtained as

$$P_{\text{qu}}^{(\text{st})}(\zeta) = |\varphi_n(\zeta)|^2. \quad (22)$$

In figures 3 and 4, we plotted $P_{\text{qu}}^{(\text{st})}(\zeta)$ (solid curves) for cases $n = 0$ and $n = 15$, respectively. For comparison purposes, the corresponding classical expressions, $P_{\text{cl}}(\zeta)$, (dotted curves) and the classical turning points (vertical dotted lines) are also shown. On the one hand, this comparison demonstrates the convergence of classical and quantum predictions for large quantum numbers. It is easy to note that there is still a large difference between two distribution functions, $P_{\text{cl}}(\zeta)$ and

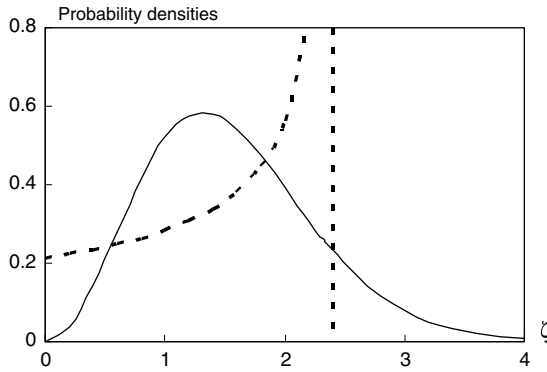


Figure 3. Classical ($P_{cl}(\zeta)$, dotted curve) and quantum ($P_{qu}^{(st)}(\zeta)$, for a particle in quantum stationary state $n = 0$, solid curve) position probability densities.

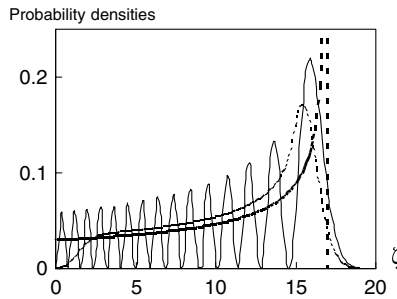


Figure 4. Classical ($P_{cl}(\zeta)$, dotted curve) and quantum ($P_{qu}^{(0)}(\zeta)$ and $P_{qu}^{(st)}(\zeta)$, for a particle in quantum stationary state $n = 15$, solid curves) position probability densities.

$P_{qu}^{(st)}(\zeta)$, due to oscillations $P_{qu}^{(st)}(\zeta)$. The same problem was discussed in Ref. [11] in connection with a harmonic oscillator. The reason of the noticeable difference being that the comparison is based on states of different quality. In fact, the probability density associated with the classical oscillation in gravitational field, whose height over the Earth is x_{\max} and which has a non-stationary state character, is compared with the position probability density of a quantum state that is stationary in character. Clearly, stationary quantum states cannot be the quantum analog of the classical state. The comparison should then be done between a classical non-stationary state and a suitable quantum non-stationary state. A suitable quantum non-stationary state is a wave packet moving in the gravitational field as the classical particle.

3.2. The wave packet in a gravitational field

In a paper by Brown and Zhang [14] a recipe is given for the construction of the explicit time development of any initial wave packet under a constant

force (without a “floor”, unlimited motion in interval $-\infty < x < +\infty$). Let us first note that the narrowest wave packet obeying the non-stationary Schrödinger equation,

$$i\hbar \frac{\partial}{\partial t} \psi(x, t) = \left(-\frac{\hbar^2}{2m} \frac{\partial^2}{\partial x^2} + mgx \right) \psi(x, t) \quad (23)$$

can be written as

$$\psi(x, t) = \exp\left(-\frac{i}{\hbar} E_1 t\right) \varphi_1(x), \quad (24)$$

where E_1 and $\varphi_1(x)$ are the first ($n = 1$) eigenvalue and eigenfunction of the stationary Schrödinger equation (16), respectively. Let us now assume that

$$\phi(x, t) = -mgxt - mg^2 t^3 / 6, \quad (25)$$

Let $\varphi_0(x)$ be the initial wave packet centered at some height, and $\varphi_0(x - v_0 t, t)$ be the description of the free-particle motion (i.e., the motion in the absence of gravitational field) with speed v_0 , then, according to Ref. [14], the wave packet

$$\psi_g(x, t) = \exp\left\{\frac{i}{\hbar} \phi(x, t)\right\} \varphi_0(x + gt^2/2, t) \quad (26)$$

will be peaked at $-gt^2/2$ and will obey the non-stationary Schrödinger equation (23), i.e., it will move as a classical particle in gravitational field [in equation (26), the initial speed, v_0 , is supposed to be equal zero]. If $\varphi_0(x)$ has a Gaussian shape, then the analytical solution for $\psi_g(x, t)$ is known [1, 16]. Indeed this wave packet, $|\psi_g(x, t)|^2$, moves as a classical particle but the width of this packet increases with time ($\sim t$). In the presence of a “floor” (i.e., a wall, $V(x) = \infty$ for $x < 0$), the time development of the wave packet changes significantly. Due to the interference of the falling and reflected parts of the wave packet, oscillations in the shape of the function $|\psi_g(x, t)|^2$ near the wall will appear [1, 15, 16]. Note that in a harmonic potential, the Gaussian wave packet moves as a classical particle and there is an initial condition for which the shape of this packet does not change with time [1, 2]. The motion of the wave packet in an infinite square well also coincides with the motion in the classical case but here the shape of wave packet changes with time [1, 4].

3.3. The zero approximation to quantum position probability density

The quantum position probability density, $P_{\text{qu}}(x)$, for the periodical motion can be calculated as [2]

$$P_{\text{qu}}(x) = \frac{2}{T} \int_0^{T/2} |\psi_q(x, t)|^2 dt. \quad (27)$$

As a zero approximation, let us suppose that the motion of a wave packet in a gravitational field in the presence of the wall is periodic and that this packet does not change its shape with time, like in the harmonic case. Here, we will assume that this wave packet has the shape of the first eigenfunction, $\varphi_1(x)$ (i.e., the initial wave packet is the narrowest), but is localized at some height above the “floor”. We will assume that this height is equivalent to some eigenvalue ζ_n (see equation (17)). Then taking into account that all the eigenfunctions $\varphi_n(\zeta) = B_n \text{Ai}(\zeta - \zeta_n)$ ($0 \leq \zeta < \infty$) are pieces of the Airy function, we get (in the variable ζ)

$$\psi_g(\zeta, t = 0) = \varphi_0(\zeta) = \begin{cases} 0, & 0 \leq \zeta < \zeta_n - \zeta_1 \\ (B_1/B_n)\varphi_n(\zeta) = B_1 \text{Ai}(\zeta - \zeta_n), & \zeta_n - \zeta_1 \leq \zeta. \end{cases} \quad (28)$$

Then according to equations (26) and (27), we have for the zero approximation

$$P_{\text{qu}}^{(0)}(x) = \frac{2}{T} \int_0^{T/2} \varphi_0^2(x + gt^2/2) dt. \quad (29)$$

Now, introducing the dimensionless time $\tau = 2t/T$ and $x_{\text{max}}^{(\text{qu})} = gT^2/8$, equation (27) can be rewritten as

$$P_{\text{qu}}^{(0)}(x) = \int_0^1 \varphi_0^2(x + x_{\text{max}}^{(\text{qu})} \tau^2) d\tau. \quad (30)$$

Finally, proceeding to the variable ζ (see, equation (17)) and taking into account the connection of the wave and Airy functions (19), we obtain

$$P_{\text{qu}}^{(0)}(\zeta) = \int_0^1 \varphi_0^2(\zeta + \zeta_{\text{max}}^{(\text{qu})} \tau^2) d\tau. \quad (31)$$

This zero approximation to quantum position probability density can be calculated numerically. In figure 2 we plotted $P_{\text{qu}}^{(0)}(\zeta)$ (solid curve) for cases $n = 15$ ($\zeta_{\text{max}}^{(\text{qu})} = 14.568$). The corresponding classical expressions, $P_{\text{cl}}(\zeta)$, (dotted curves) and the classical turning point, $\zeta_{\text{max}}^{(\text{cl})} = \zeta_{15}$, (vertical dotted line) are also shown. The used value for $\zeta_{\text{max}}^{(\text{qu})}$ corresponds to the quantum number $n = 15$ and was obtained in the following way: at time $t = T/2$ (or at $\tau = 1$), the initial wave packet (28) is coincident with the first eigenfunction, $\varphi_1(\zeta) = B_1 \text{Ai}(\zeta - \zeta_1)$, i.e., $B_1 \text{Ai}(\zeta + \zeta_{\text{max}}^{(\text{qu})} \tau^2 - \zeta_n) |_{\tau=1} = B_1 \text{Ai}(\zeta - \zeta_1)$, and in this case, $\zeta_{\text{max}}^{(\text{qu})} + \zeta_1 = \zeta_{15}$. The difference between $\zeta_{\text{max}}^{(\text{qu})}$ and ζ_{15} reflects the fact that the minimum energy of quantum particle in the gravitational field with “floor” is equal E_1 (or ζ_1 in dimensionless variables). Figure 2 allows a direct comparison between the classical position distribution and the zero approximation to the quantum distribution.

3.4. The approximate quantum position probability density

Let us write the wave function (the wave packet) (26) as a superposition (with coefficients C_k) of the stationary states (19) of the oscillator in the gravitational field,

$$\psi_g(x, t) = \sum_k C_k \varphi_k(x) \exp\left(-\frac{1}{\hbar} E_k t\right). \quad (32)$$

Then

$$|\psi_g(x, t)|^2 = \sum_{m,k} C_m C_k^* \varphi_m(x) \varphi_k^*(x) \exp\left(-\frac{1}{\hbar} (E_m - E_k) t\right). \quad (33)$$

For the quantum position probability density, we obtain

$$P_{\text{qu}}(x) = \lim_{T_0 \rightarrow \infty} \frac{1}{T_0} \int_0^{T_0} |\psi_g(x, t)|^2 dt = \sum_k |C_k|^2 \varphi_k^2(x). \quad (34)$$

As the probability density $P_{\text{qu}}(x)$ has to be normalized, the coefficients C_k will obey the condition: $\sum_k |C_k|^2 = 1$.

For the full time-dependent solution (32) one needs the expansion coefficients C_k , which depend on the initial condition. Assuming, for the expansion coefficients C_k , the initial condition of equation (28), we will have

$$C_k = \int_0^\infty \varphi_k(\zeta) \psi_g(\zeta, 0) d\zeta = B_1 \int_{\zeta_n - \zeta_1}^\infty \varphi_k(\zeta) Ai(\zeta - \zeta_n) d\zeta. \quad (35)$$

Coefficients C_k were calculated numerically, their values are shown in table 1. At the initial conditions of equation (28), we can suppose that the dominant term in the series (34) is the term with $k = n$. Thus, as a first crude approximation we can write (introducing again the dimensionless parameter, ζ)

$$P_{\text{qu}}(\zeta) \approx P_{\text{qu}}^{(\text{st})}(\zeta) = \varphi_n^2(\zeta). \quad (36)$$

This function is shown in figure 4 for $n = 15$. If we include in the approximation the terms with index $k = n \pm 1$ and provide for the correct normalization, then the approximation, $P_{\text{qu}}^{(3)}(\zeta)$, to relation (34) becomes

$$P_{\text{qu}}(\zeta) \approx P_{\text{qu}}^{(3)}(\zeta) = (|C_{n-1}|^2 + |C_n|^2 + |C_{n+1}|^2)^{-1} \sum_{i=-1}^1 |C_{n+i}|^2 \varphi_{n+i}^2(\zeta) \quad (37)$$

what, according to figure 5 ($n = 15$), approaches to equation (15) somewhat better than equation (36).

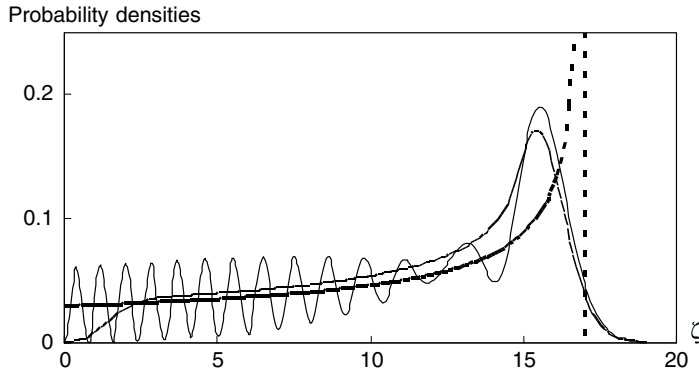


Figure 5. Classical ($P_{cl}(\zeta)$, dotted curve) and quantum ($P_{qu}^{(0)}(\zeta)$, dashed curve, and $P_{qu}^{(3)}(\zeta)$, $C_{14} = 0.5065$, $C_{15} = 0.6129$, $C_{16} = 0.4611$, solid curve) position probability densities.

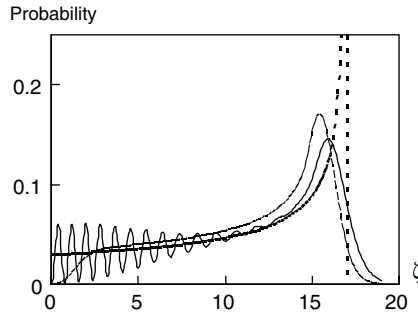


Figure 6. Classical ($P_{cl}(\zeta)$, dotted curve) and quantum ($P_{qu}^{(0)}(\zeta)$, dashed curve, and $P_{qu}^{(7)}(\zeta)$, $C_{12} = 0.1316$, $C_{13} = 0.2980$, $C_{14} = 0.5065$, $C_{15} = 0.6129$, $C_{16} = 0.4611$, $C_{17} = 0.1118$, $C_{18} = -0.1224$, solid curve) position probability densities.

If we yet include the terms with indexes $k = n \pm 2, n \pm 3$ and provide, again, for the correct normalization, we obtain the approximation $P_{qu}^{(7)}(\zeta)$,

$$P_{qu}(\zeta) \approx P_{qu}^{(7)}(\zeta) = \left(\sum_{i=-3}^3 |C_{n+i}|^2 \right)^{-1} \sum_{i=-3}^3 |C_{n+i}|^2 \varphi_{n+i}^2(\zeta). \quad (38)$$

According to figure 6 ($n = 15$), the probability density $P_{qu}^{(7)}(\zeta)$ approaches to equation (15) somewhat better than equation (37). Including more and more terms, we would eventually approach the exact position probability density (34). Note that the other coefficients are rather small ($|C_{n \pm i}| < 0.1$ for $n = 15$ and $i > 3$). Our calculations show that their inclusion (up to $i = 10$) into series (34) does not noticeably change the approximation (38). It seems that the probability density $P_{qu}^{(7)}(\zeta)$ gives the correct approximation to (34). The oscillations near the wall (“floor”) reflect the interference of falling and reflected waves. These oscillations can also be seen

throughout the figures of wave packet propagation in gravitational field near the wall (i.e., see figures 3 and 4 in Ref. [15] and figure 1 in Ref. [16]).

For larger energies (larger n , classical limit), the amplitude of oscillation of Airy functions near the wall decreases [22,23], so the quantum and classical position probability functions become increasingly similar (with the exception of the space interval near the classical turning points).

4. Conclusions

Many interesting conclusions can be drawn from these results. First of all, comparison between the classical and the quantum case obliges to differentiate between two different quantum cases (a) a quantum stationary case and (b) a quantum non-stationary case. This last case, then, allows for two approximate solutions (a) the zero approximation to the quantum position probability density, where the wave packet has the shape of the first eigenfunction, and (b) a more general approximate solution to the quantum position probability function, where the wave packet is a superposition of several stationary states. A direct comparison among the four cases for the position probability function, i.e., the classical case, the stationary quantum case, the non-stationary quantum zero case, and the non-stationary quantum superposition case, let us conclude that (i) the classical case shows, as usual, that the probability density is peaked at the turning point, where the speed of the particle is zero (figure 2, dotted line). The (ii) quantum stationary case shows that (a) it diverges from the classical solution at the reflection point, where oscillations are evident and (b) at the classical turning point, where the particle can penetrate through the potential barrier (figure 4, the wavy-line). The (iii) quantum non-stationary zero case, even if it is a rather crude approximation, as it does not include the interference of the falling and reflected waves, shows a quantitative agreement with the previous quantum case in the mid-distance and near the classical turning point (figure 4, solid non-wavy-line). The (iv) quantum non-stationary superposition case shows that in the mid-distances it resembles the classical case, while at the classical turning point it show the well-known quantum penetration through the barrier, and at the short-distances, near the “floor”, shows the existence of interference between falling and reflected waves (figure 6, wavy-line). Further, when the energy of quantum particle increases the quantum superposition solution seems to approach the classical case, because the amplitude of the oscillations decrease near the “floor” and the width of quantum distribution near the classical turning point decreases in comparison to the full allowed distance of the motion (x_{\max}).

5. Bibliographical note

George Biddell Airy was born on July 27, 1801 and died on January 2, 1892. He was the seventh Astronomer Royal from 1835 to 1891 and a very

versatile scientist. For his scientific achievements he was knighted in 1872. He reorganized the Royal Greenwich Observatory. Airy improved the theory of orbital motions of Venus and of the Moon. In 1827 he did the first attempt to correct astigmatism in the human eye by use of a cylindrical eyeglass lens. In 1838 he devised a compass-correction system for the Royal Navy. In 1854 he measured gravity by swinging a pendulum at the top and at the bottom of a deep mine and thus computed the density of the Earth. We should note that the value he obtained was too large by a fair amount. In 1871 he used a water-filled telescope to test the effect of the Earth's motion on the aberration of light. He contributed also, in optics, to the study of interference fringes and to mathematical theory of rainbows. The Airy disk, the central spot of light in the diffraction pattern of a point light source, is named after him. He was among the first to propose (c. 1855) the theory that root structures of lower density must exist under mountains to maintain isostatic equilibrium. Airy went on a number of scientific expeditions to study the eclipse including Turin in 1842, Sweden in 1851 and Spain in 1860. He was an opponent of Charles Babbage. When the Government was considering funding Babbage's calculating engine, the Government asked Airy what would be the value of such a device. Airy answered with one word: worthless.

The Airy function is the solution of differential equation:

$$y'' - xy = 0. \quad (39)$$

There are two independent solutions: $Ai(x)$ approaches to zero for large x , and $Bi(x)$ goes to infinity for larger x . The Airy function is found as solution to boundary value problems in quantum mechanics and electromagnetic theory. The story of this function starts in France. It was known that France was building a new huge telescope. The French instrument, actually, was so overweight that its longitudinal axis was deflected into a curve which affected more than heavenly bodies and thus rendered the telescope useless. When Airy knew about this problem he immediately wrote out something about it: *a state of plane strain in a two-dimensional solid, free from body forces, may be specified by three mutually orthogonal stress components. These may be stated as first-order differential equation. If the three stress components are equal to the appropriate second order partial derivatives of an arbitrary function, then satisfy the equilibrium conditions.* In spite of the fact that Airy spoke in italics he was well-understood for the function to be called an Airy function.

References

- [1] S. Brandt and H.D. Dahmen, in: *The Picture Book of Quantum Mechanics* (Wiley, New York, 1985).
- [2] C. Leubner, M. Alber and N. Schupfer, *Am. J. Phys.* 56 (1988) 1123.
- [3] R.W. Robinett, *Am. J. Phys.* 65 (1997) 190.
- [4] R. Bluhm, V.A. Koctelecký and J.A. Porter, *Am. J. Phys.* 64 (1996) 944.

- [5] M.N. Berberan-Santos, E.N. Bodunov and L. Pogliani, Am. J. Phys. 65 (1997) 404.
- [6] F.G.E. Pantellini, Am. J. Phys. 68 (2000) 61.
- [7] M.N. Berberan-Santos, E.N. Bodunov and L. Pogliani, Am. J. Phys. 70 (2002) 438.
- [8] R.L. Gibbs, Am. J. Phys. 43 (1975) 25.
- [9] V.C. Aguilera-Navarro, H. Iwamoto, E. Ley-Koo and A.H. Zimmerman, Am. J. Phys. 49 (1981) 648.
- [10] R.D. Desko and D.J. Bord, Am. J. Phys. 51 (1983) 82.
- [11] D.A. Goodins and T. Szeredi, Am. J. Phys. 51 (1991) 924.
- [12] H. Wallis, J. Dalibard and C. Cohen-Tannoudji, Appl. Phys. B 54 (1992) 407.
- [13] S. Whineray, Am. J. Phys. 60 (1992) 946.
- [14] L.S. Brown and Y. Zhang, Am. J. Phys. 62 (1994) 806.
- [15] J. Gea-Banacloche, Am. J. Phys. 67 (1999) 776.
- [16] M.A. Doncheski and R.W. Robinett, Am. J. Phys. 69 (2001) 1084.
- [17] O. Halpern, Phys. Rev. 86 (1952) 126 and 87 (1952) 520.
- [18] H.A. Gersch, J. Chem. Phys. 27 (1957) 928.
- [19] V.V. Nesvizhevsky, H.G. Börner, A.K. Petuhov, H. Abele, S. Baeßler, F.J. Rueß, T. Stöferle, A. Westphal, A.M. Gadarski, G.A. Petrov and A.V. Strelkov, Nature 415 (2002) 297.
- [20] J.P. Dowling and J. Gea-Banacloche, Adv. At. Mol. Opt. Phys. 37 (1996) 1.
- [21] P. Dennery and A. Krzywicki, in: *Mathematics for Physicists* (Harper & Row, New York, 1967), p. 237.
- [22] M.A. Abramovitz and I.A. Stegun, in: *Handbook of Mathematical Functions* (Dover, New York, 1972).
- [23] E. Jahnke and F. Emke, in: *Tables of Functions* (Dover, New York, 1945).